Title
Impacts of Subsurface Tile Drainage on Age—Concentration Dynamics of Inorganic Nitrogen in Soil

Journal
Water Resources Research, 55(2)

ISSN
0043-1397

Authors
Woo, Dong K
Kumar, Praveen

Publication Date
2019-02-01

DOI
10.1029/2018wr024139

Peer reviewed

Water Resources Research

RESEARCH ARTICLE
10.1029/2018WR024139

Special Section:
Dynamics in Intensively Managed Landscapes: Water, Sediment, Nutrient, Carbon, and Ecohydrology

Impacts of Subsurface Tile Drainage on Age—Concentration Dynamics of Inorganic Nitrogen in Soil

Dong K. Woo[1,2] **and Praveen Kumar**[1,3]

[1]Department of Civil and Environmental Engineering, University of Illinois at Urbana-Champaign, Urbana, IL, USA,
[2]Now at Lawrence Berkeley National Laboratory, Berkeley, CA, USA,
[3]Department of Atmospheric Sciences, University of Illinois at Urbana-Champaign, Urbana, IL, USA

Key Points:
- The high concentration and low age of nitrate are observed in areas near tile drains
- The age of inorganic soil nitrogen in the fracture is not always lower than that in the matrix
- Our results can contribute to precision agriculture practices for nitrogen applications to reduce environmental impacts

Correspondence to:
P. Kumar,
kumar1@illinois.edu

Citation:
Woo, D. K., & Kumar, P. (2019). Impacts of subsurface tile drainage on age–Concentration dynamics of inorganic nitrogen in soil. *Water Resources Research*, *55*, 1470–1489. https://doi.org/10.1029/2018WR024139

Received 20 SEP 2018
Accepted 16 JAN 2019
Accepted article online 22 JAN 2019
Published online 21 FEB 2019

Abstract We explore the impacts of tile drains in agricultural fields on the coupled age and concentration dynamics of nitrate, immobile ammonium, mobile ammonia and ammonium, and nonreactive tracers such as chloride. We implement two mobile interacting pore domains to capture matrix and preferential flow paths in a coupled ecohydrology and biogeochemistry model, *Dhara*. We apply this model to an agricultural farm that utilizes a corn-soybean rotation in the Midwestern United States located in the Intensively Managed Landscapes Critical Zone Observatory. In general, we observe both low concentration and age of nitrate in the areas that are classified as topographic depressions even with the presence of tile drains. Also, an increase in the age of mobile ammonia/ammonium is observed after installing tile drains. This is in contrast to the cases for nitrate, immobile ammonium, and nonreactive tracer. These results arise because the depletion of mobile ammonia/ammonium due to tile drainage causes a high mobility flux from immobile ammonium to mobile ammonia/ammonium, which also carries a considerable amount of relatively old age of nitrogen from immobile ammonium to mobile ammonia/ammonium. These results illustrate how storm event scale dynamics impact spatial heterogeneity and temporal variability of the efflux, which helps in disentangling the complexity of nitrogen dynamics in the soil. This understanding can contribute to precision agriculture for nitrogen applications to reduce environmental impacts.

Plain Language Summary Age-concentration dynamics for inorganic nitrogen in the soil characterizes for how long and how much nitrogen is present in the soil and how these vary in space and time. This paper shows how the presence of subsurface tile drains, a dominant hydrologic control in the midwestern United States and many other parts of the world, structures this variability. It also argues that using traditional tracer methods, such as chloride and bromide, does not capture the longer residence of nitrogen in the soil due to its complex reactive nature in the soil. By understanding what controls these variabilities, we can develop new methods for reducing the application of fertilizers.

1. Introduction

Glacial deposit overlain by loess has resulted in a low gradient landscape with high water retention capacity in the U.S. Midwest. Organically rich soil in this region supports highly productive agriculture, made possible, in part, from the extensive deployment of a network of tile drains at a depth of ~1.5 m (Du et al., 2005; de la Cretaz & Barten, 2007) across this vast region. These drains, initially built from perforated earthen tubes and with polyvinyl chloride more recently, allow moisture to quickly drain from the soil above the tile. This creates an unsaturated zone, which would be otherwise water logged, which is better suited for seed germination and growth of agricultural crops. It also allows for farm machinery to enter the agricultural farms earlier in the spring season, thereby extending the length of the growing period (Dinnes et al., 2002; Skaggs et al., 1994). These tile networks also increase the connectivity between landscape and channels by providing a rapid flow pathway for the movement of moisture and other dissolved constituents such as nitrate, ammonia, and ammonium. Since the agricultural system relies heavily on fertilizer application, it should be expected that the tile network would be an important control on the spatial heterogeneity of the distribution of concentration and age of nitrogen in the soil. Further, this spatial heterogeneity would also determine the age of nitrogen in the efflux through the tile drain.

Age of inorganic nitrogen is an estimate of the elapsed time since it is introduced into the soil matrix. The inorganic nitrogen molecules can enter by atmospheric deposition, mineralization of organic substrate such as dead root and litter, or fertilizer application. These are considered as birth processes, and the time elapsed since a nitrogen molecule of any chemical species such as nitrate, ammonia, or ammonium enters the soil through any of these mechanisms is its age (Woo & Kumar, 2016, 2017). While studies have documented the role and impact of tile drains as rapid conduit for loss of nitrogen to receiving water bodies resulting in adverse environmental impacts (Buyuktas et al., 2004; Dusek et al., 2008; Filipovic et al., 2014; Gentry et al., 1998; Gerke et al., 2007; Mohanty et al., 1998; Sands et al., 2008), little is known about how they shape the spatial heterogeneity of concentration and age of nitrogen through the soil column. This heterogeneity is further modulated by topographic variability, such as the presence of microtopographic depressions (Le & Kumar, 2014; Woo & Kumar, 2017) where ponding creates additional hydraulic head that increases nitrogen transport and reduces mean age by moving younger molecules from near surface to deeper layers. In this paper we use numerical simulation, based on the theory of mean age (henceforth "age"; Woo & Kumar, 2016), to characterize dependencies between concentration and age, and their spatial distribution as an outcome of the coupled interaction between the control of microtopographic variability on the surface and tile drains in the soil below. This paper builds on prior work (Woo & Kumar, 2016, 2017) by explicitly incorporating and considering the spatial network of tile drains. Further, we incorporate macropore flow using a dual-permeability model in the age-concentration formulation of inorganic nitrogen dynamics, thereby expanding the applicability of age-concentration characterization.

Since the extensive tile drainage network controls the nitrogen cycle in agricultural systems (de la Cretaz & Barten, 2007; Fausey et al., 1995; Radcliffe et al., 2015), its influence on nitrogen dynamics plays a key role in determining the short- and long-term evolution of soil inorganic nitrogen concentration and age. Several studies (e.g., Duffy, 2010; Goode, 1996; Turnadge & Smerdon, 2014) have noted that the combined analysis of concentration and age of nonreactive chemical constituents provides a better understanding of a given system. While concentration provides a snapshot of a given dynamics on the basis of on-going interactions (Delhez et al., 2004), age reflects the accumulated temporal history of fluxes, transport, and transformation. This is especially important for a reactive substance, such as nitrogen, because different nitrogen species are impacted by different physical and chemical properties in the soil. For example, nitrate being soluble can be mobilized more easily than ammonium, whose mobility through the soil may be limited due to its positive charge that creates a stronger bond with clay minerals. However, when nitrogen from one species is chemically transformed to another (e.g., the conversion of ammonium to nitrate through nitrification), it carries its age with it. Thus, the age of nitrate is influenced not only by the flow properties of the system but also the factors that control the chemical transformation between different species. This feature of age conveyance between different chemical species enables a better assessment of the complex dynamics of soil inorganic nitrogen as a whole by providing interdependent characterization of concentration and age. This is in contrast to conventional approaches, such as the assessment of residence time using inflow-outflow analysis (Bolin & Rodhe, 1973) and experimental use of nonreactive tracer as a substitute for reactive tracer (Zarnetske et al., 2011). The spatial mapping to nitrogen concentration and age under tile-drained fields has the potential to open up novel solution to the vexing challenge of reducing environmental impacts while at the same time maintaining agricultural productivity. Precision agricultural practices for nutrient management can be developed that target applications in areas of low concentration and age, with reduced applications in areas that exhibit high concentration and age.

This paper is organized as follows. First, we describe the study site and the mathematical formulations associated with the 3-D spatial simulation of flow and nitrogen dynamics through a tile drains soil system. We then describe the results followed with summary and discussions.

2. Study Site

We study the impacts of tile drainage on the distribution of concentration and age of inorganic soil nitrogen for the case of a private farm near DeLand, Illinois, United States (40° 09′ 55.44″N, 88° 39′ 20.30″W, and ~216 m above sea level). This site in the Intensively Managed Landscape-Critical Zone Observatory is an agricultural field with the cultivation of corn-soybean through rotation, a common agricultural practice in the Midwestern United States. The plot was planted with soybean in May 2007 and with corn in May 2008. The soil type is primarily silty clay loam. Nitrogen fertilizer was only applied to corn at 15.2 g/m^2 (Woli et al., 2010). For this site, tile drains were installed at a depth of 1.2 m in autumn of 2003 (Woli et al., 2010).

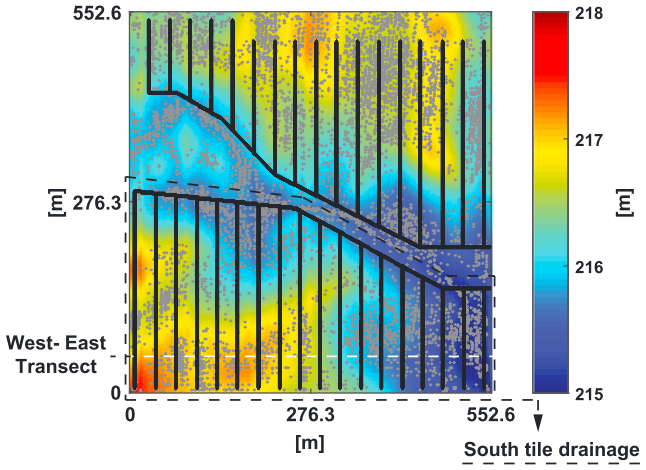

Figure 1. Tile drain map (black line) is overlaid on the elevation map (height above mean sea level) of the study site. The spacing between tiles is approximately 30 m. The drainages in north and south plots (black dashed line) occur independently. The gray dots represent topographic depressions. The white dashed line denotes the cross-sectional area where vertical and temporal variabilities in inorganic soil nitrogen concentration and its age are evaluated.

The installed tiles constitute two independent networks (see Figure 1) hereafter referred as northern and southern networks. The 1.8-m LiDAR digital elevation data obtained from Illinois State Geological Survey (https://www.isgs.illinois.edu) along with the tile drain map (black lines) are shown in Figure 1.

For simulation the forcing data, such as precipitation, atmospheric pressure, air temperature, incoming shortwave radiation, humidity, wind speed, and vapor pressure, are obtained from a nearby site from National Solar Radiation Database (http://rredc.nrel.gov) and National Oceanic and Atmospheric Administration (https://www.ncdc.noaa.gov). The data from the years 1994 to 2003 are used for a model spinup with observed carbon and nitrogen concentration data from an adjacent field, which is the only available data, as the starting condition. This strategy provides a reasonable time frame for transients related to the initial conditions to die out. Subsequent to this, simulations for 2004 to 2010 were performed with tile drains. This study presents results for the period from 2007 to 2010 to allow time for the suppression of transients in the observation from excavation related to the installation of tiles in autumn of 2003.

For the purpose of comparison between the age of the reactive nitrogen species to that of a nonreactive tracer, such as chloride or bromide that are typically used as tracers, we also estimate the concentration and age of the latter. It is noted that we are not striving to simulate the age dynamics of chloride or bromide but rather to attempt to use them as a reference to compare and contrast the age of nonreactive tracer against that of reactive tracer, inorganic nitrogen in this study. The dynamics of both reactive and nonreactive tracer are assumed to be passive and not to alter the soil water flow characteristics. We assume that infiltration into the soil has a constant concentration of 1 g/m^3 of nonreactive tracer consistent with prior studies in (Woo & Kumar, 2016, 2017).

3. Age-Concentration Dynamics in Dual-Permeability Soil

We draw upon the formulation of age-concentration dynamics of inorganic nitrogen presented in Woo and Kumar (2016, 2017) and extend it to consider dual permeability to account for macropore flow in the soil. Soil macropores or macrostructures, such as cracks, fissures, and earthworm and root channels, play an important role in agricultural soils (Kohler et al., 2001; Stone & Wilson, 2006; Williams et al., 2016). In particular, preferential flow paths can act as rapid transport pathways of young inorganic nitrogen present in topsoil into subsurface tile drains, reducing overall age and concentration of inorganic nitrogen in the soil. It is shown that the preferential transport of soil nitrate is dominant under saturated soil conditions (Chen et al., 2001), which corresponds to the timing of tile flow events (Arnold et al., 1999; Green et al., 2006).

3.1. Ecohydrologic Model

The dual-permeability model to describe soil moisture, temperature, and nutrient in two mobile interacting pore domains is incorporated by modifying a coupled ecohydrological and biogeochemical dynamics model, *Dhara* (Le & Kumar, 2017; Woo & Kumar, 2017). The variables predicted from the ecohydrological model, such as plant water uptake, subsurface water fluxes, and soil moisture and temperature are used to drive the biogeochemical model including inorganic nitrogen age dynamics that will be discussed in section 3.2. The 3-D subsurface moisture flow is modeled using two coupled Richards' equations for the fracture (subscript f) and the matrix (subscript m; Gerke & van Genuchten, 1993a, 1993b):

$$S_{s,f}\frac{\theta_f}{\phi_f}\frac{\partial \psi_f}{\partial t}+\frac{\partial \theta_f}{\partial t}=\Delta\cdot K_f\left(\theta_f\right)\left[\Delta\psi_f+\hat{k}\right]+q_{s,f}+q_{e,f}-\frac{\Gamma_w}{w_f} \tag{1}$$

and

$$S_{s,m}\frac{\theta_m}{\phi_m}\frac{\partial \psi_m}{\partial t}+\frac{\partial \theta_m}{\partial t}=\Delta\cdot K_m\left(\theta_m\right)\left[\Delta\psi_m+\hat{k}\right]+q_{s,m}+q_{e,m}+\frac{\Gamma_w}{w_m}, \tag{2}$$

where $S_{s,f}$ and $S_{s,m}$ are specific storage coefficients of the fracture and matrix (m^{-1}), respectively; θ_f and θ_m are soil moistures of the fracture and matrix (m^3/m^3), respectively; ψ_f and ψ_m are subsurface water pressure heads in the fracture and matrix (m), respectively; ϕ_f and ϕ_m are porosities of the fracture and matrix (−), respectively; K_f and K_m are unsaturated hydraulic conductivities in the fracture and matrix (m/hr), respectively; $\hat{k}$ is the unit upward vector; $q_{s,f}$ and $q_{s,m}$ represent the general source/sink term such as plant water uptake in the fracture and matrix (m/hr); $q_{e,f}$ and $q_{e,m}$ are exchange fluxes of the fracture and matrix (m/hr), respectively, between the 2-D surface and 3-D subsurface domains, such as infiltration; w_f and w_m are the relative volumetric fraction of the fracture and matrix (−); and Γ_w is the interdomain water exchange between the fracture and matrix (hr^{-1}). Γ_w is estimated as

$$\Gamma_w = \frac{\beta}{a_w^2}\gamma_w K_w(\psi_f - \psi_m), \tag{3}$$

where β_w, a_w, γ_w, and K_w are a geometry-dependent factor (−), average length between the two regions (m), scaling factor (−), and saturated hydraulic conductivity of the interface between the two regions (m/hr), respectively (Gerke & van Genuchten, 1993a, 1993b). The volume-weighted soil moisture of the bulk soil (θ) is represented as

$$\theta = w_f\theta_f + w_m\theta_m. \tag{4}$$

The 3-D subsurface temperature is modeled using the heat diffusion equation based on Vogel et al. (2011):

$$C_{T,f}\left(\theta_f\right)\frac{\partial T_{s,f}}{\partial t} = \Delta \cdot K_{T,f}\left(\theta_f\right)\left[\Delta T_{s,f}\right] - \frac{\Gamma_T}{w_f} \tag{5}$$

and

$$C_{T,m}\left(\theta_m\right)\frac{\partial T_{s,m}}{\partial t} = \Delta \cdot K_{T,m}\left(\theta_m\right)\left[\Delta T_{s,m}\right] + \frac{\Gamma_T}{w_m}, \tag{6}$$

where $T_{s,f}$ and $T_{s,m}$ are soil temperatures of the fracture and matrix (K), respectively; $C_{T,f}$ and $C_{T,m}$ are volumetric heat capacities in the fracture and matrix ($J{\cdot}m^{-3}{\cdot}K^{-1}$), respectively; and $K_{T,f}$ and $K_{T,m}$ are thermal conductivities in the fracture and matrix ($W{\cdot}m^{-1}{\cdot}K^{-1}$), respectively. Γ_T is the interdomain heat exchange between the fracture and matrix (K/hr) and is estimated as

$$\Gamma_T = \Gamma_w c_w T_{s,w} + \alpha_T(T_{s,f} - T_{s,m}), \tag{7}$$

where c_w is the volumetric heat capacity of water ($J{\cdot}m^{-3}{\cdot}K^{-1}$). In case that the direction of water is from the matrix to the fracture, $T_{s,w} = T_{s,m}$, and in the opposite case, $T_{s,w} = T_{s,f}$. α_T is a heat exchange coefficient ($W{\cdot}m^{-3}{\cdot}K^{-1}$) and is estimated as

$$\alpha_T = \wp K_{T,T}, \tag{8}$$

where $\wp$ is the interdomain heat transfer coefficient (m^{-2}). We assume that the thermal conductivity for the interdomain heat exchange is controlled by the minimum of the fracture and matrix domain conductivity, which is $K_{T,T} = \min\left\{K_{T,f}, K_{T,m}\right\}$. Parameters used in this study are presented in Table 1.

3.2. Mean Age Model for Inorganic Soil-Nitrogen in a Dual-Permeability Soil

Since age is the time elapsed since a chemical constituent is introduced into a control volume (Danckwerts, 1953), the gain of chemical constitute from the outside of a control volume increases the concentration but decreases the mean age (τ [day]). On the other hand, the loss of chemical constituents out of the control volume will decrease the concentration but change the age depending on the age of the chemical constituents in the efflux. Because of arrival and/or loss, at each time step (t [day]), the concentration ($c_i(t, \mathbf{x}, \tau)$ [$g{\cdot}m^{-3}{\cdot}day^{-1}$]) of a chemical species i is comprised of molecules that have an age distribution. That is, the concentration density is not only a function of time (t) and location ($\mathbf{x}$) but also age (τ). For this study, c_i can be nitrate in the fracture (n_f^- [$g{\cdot}m^{-3}{\cdot}day^{-1}$]) and matrix ($n_m^-$ [$g{\cdot}m^{-3}{\cdot}day^{-1}$]), immobile ammonium in the fracture ($n_{im,f}^+$ [$g{\cdot}m^{-3}{\cdot}day^{-1}$]) and matrix ($n_{im,m}^+$ [$g{\cdot}m^{-3}{\cdot}day^{-1}$]), and mobile ammonia/ammonium in the

Table 1
Parameters for the Tile Drain Model

Parameters and descriptions	Value
Horizontal mesh size, $\Delta x = \Delta y$ (m)	1.8
Vertical mesh size, Δz (m)	0.2
Time step, Δt (hr)	1
Ecohydrological parameters	
Fracture	
vanGenuchten - Alpha (cm^{-1})	0.027 (Leij et al., 1996)
vanGenuchten - Pore size distribution (−)	3.00 (Vogel et al., 2011)
Specific storage (m^{-1})	0.0005 (Le et al., 2015)
Saturated soil moisture (m^3/m^3)	0.6 (Vogel et al., 2011)
Residual soil moisture (m^3/m^3)	0.01 (Vogel et al., 2011)
Saturated hydraulic conductivity (m/hr)	0.08 (Vogel et al., 2011)
Relative volumetric fraction, w_f (−)	0.2 (Othmer et al., 1991)
Matrix	
vanGenuchten - Alpha (cm^{-1})	0.027 (Leij et al., 1996)
vanGenuchten - Pore size distribution (−)	1.41 (Leij et al., 1996)
Specific storage (m^{-1})	0.0005 (Le et al., 2015)
Saturated soil moisture (m^3/m^3)	0.55 (Leij et al., 1996)
Residual soil moisture (m^3/m^3)	0.1 (Leij et al., 1996)
Saturated hydraulic conductivity (m/hr)	0.0061 (Guarracino, 2007)
Relative volumetric fraction, w_m (−)	0.8 (Othmer et al., 1991)
Geometry-dependent factor, β (−)	0.45 (Arora et al., 2012)
Average length between the two regions, a (m)	0.1195 (Arora et al., 2012)
Scaling factor, γ_w (−)	0.001 (Arora et al., 2012)
Saturated hydraulic conductivity of the interface, K_w (m/hr)	0.0026 (Arora et al., 2012)
Inter-domain heat transfer coefficient, $\wp$ (m^{-2})	1 (Vogel et al., 2011)
Biogeochemical parameters	
Nitrate diffusion coefficient (m^2/day)	0.000017 (Canter, 1997)
Ammonia/ammonium diffusion coefficient (m^2/day)	0.0000013 (Canter, 1997)
Fertilizer amount (gN/m^2)	15.2 (Woli et al., 2010)
Fertilizer application date (DOY)	130 (Woo & Kumar, 2017)
Tile drain parameters	
Tile drain hydraulic conductivity, K_T (m/hr)	5 (Freeze & Cherry, 1979)
Tile flow trigger threshold pressure head, ψ_{tr} (m)	0
Effective drain spacing, d_e (m)	30 (Shen et al., 1998)

Note. Parameters not presented in this table are described in Woo and Kumar (2017).

fracture ($n_{mo,f}$ [$g{\cdot}m^{-3}{\cdot}day^{-1}$]) and matrix ($n_{mo,m}$ [$g{\cdot}m^{-3}{\cdot}day^{-1}$]). Using $dc_i = \frac{\partial c_i}{\partial t}dt + \frac{\partial c_i}{\partial \tau}dt$ and noting that $\frac{\partial c_i}{\partial \tau} = 1$ since age changes at the same rate as time, this dynamics can be written as

$$\frac{dc_i}{dt} = \frac{\partial c_i}{\partial t} + \frac{\partial c_i}{\partial \tau} = \text{gain rate - loss rate} \\ -\text{divergence of advective mass flux} \tag{9}$$

where the term, $\frac{\partial c_i}{\partial \tau}$, is the age flux. Diffusion or dispersion is assumed to be small and is not considered so that the transport is governed by advection. Gain and loss rates represent transformations, such as mineralization, nitrification, and plant and microbial uptake.

The gain terms of nitrate in the fracture (n_f^- [$g{\cdot}m^{-3}{\cdot}day^{-1}$]) considered are nitrate input from surface ($e_{e,f}^-$ [$g{\cdot}m^{-3}{\cdot}day^{-2}$]) that includes fertilizer application and atmospheric deposition, and nitrification

from immobile ammonium ($\frac{\xi_{im}^+}{\xi^-} o_{im,f}$ [g·m^{-3}·day^{-2}]) and from mobile ammonia/ammonium ($\frac{\xi_{mo}^+}{\xi^-} o_{mo,f}$ [g·m^{-3}·day^{-2}]), where ξ^-, ξ_{im}^+, and ξ_{mo}^+ are the volumetric fraction of nitrate, immobile ammonium, and mobile ammonia or ammonium, respectively. The loss terms of nitrate in the fracture are nitrate crop uptake (p_f^- [g·m^{-3}·day^{-2}]) and microbial uptake (l_f^- [g·m^{-3}·day^{-2}]), N_2O production by nitrification (q_f [g·m^{-3}·day^{-2}]), denitrification (j_f [g·m^{-3}·day^{-2}]), and nitrate in tile flow (g_f^- [g·m^{-3}·day^{-2}]). For the case of the matrix, the same gain and loss terms are used with subscript m instead of subscript f. By considering the divergence of advective mass flux, age flux, and the nitrate mass exchange flux between the fracture and matrix (Γ_n^- [g·m^{-3}·day^{-2}]), we get

$$\frac{\partial n_f^-}{\partial t} + \frac{\partial n_f^-}{\partial \tau} = \left(e_{e,f}^- + \frac{\xi_{im}^+}{\xi^-} o_{im,f} + \frac{\xi_{mo}^+}{\xi^-} o_{mo,f} \right) - (p_f^- + l_f^- + q_f + j_f + g_f^-) - \Delta \cdot \left(\vec{u}_f \frac{n_f^-}{\theta_f} \right) - \frac{\Gamma_n^-}{w_f} \tag{10}$$

and

$$\frac{\partial n_m^-}{\partial t} + \frac{\partial n_m^-}{\partial \tau} = \left(e_{e,m}^- + \frac{\xi_{im}^+}{\xi^-} o_{im,m} + \frac{\xi_{mo}^+}{\xi^-} o_{mo,m} \right) - (p_m^- + l_m^- + q_m + j_m + g_m^-) - \Delta \cdot \left(\vec{u}_m \frac{n_m^-}{\theta_m} \right) + \frac{\Gamma_n^-}{w_m}, \tag{11}$$

where

$$\Gamma_n^- = \Gamma_w \frac{n_w^-}{\theta_w} + \frac{\beta}{a^2} D^- (n_f^- - n_m^-) \tag{12}$$

and $\vec{u_f}$ and $\vec{u_m}$ are the velocity of the subsurface water flow in the fracture and matrix (m/day), respectively. In case that the direction of water is from the matrix to the fracture, $n_w^- = n_m^-$ and $\theta_w = \theta_m$, and in the opposite case, $n_w^- = n_f^-$ and $\theta_w = \theta_f$. D^- is a nitrate diffusion coefficient (m^2/day).

The loss of immobile ammonium in the fracture ($n_{im,f}^+$ [g·m^{-3}·day^{-1}]) arises from microbial uptake ($l_{im,f}^+$ [g·m^{-3}·day^{-2}]) and nitrification ($o_{im,f}$ [g·m^{-3}·day^{-2}]). There is a mobility flux between the immobile ammonium and mobile ammonia/ammonium (r_f [g·m^{-3}·day^{-2}]). For the case of the matrix, the same loss and mobility flux terms are used with subscript m instead of subscript f. By considering the age flux, we get

$$\frac{\partial n_{im,f}^+}{\partial t} + \frac{\partial n_{im,f}^+}{\partial \tau} = -(l_{im,f}^+ + o_{im,f}) + r_f \tag{13}$$

and

$$\frac{\partial n_{im,m}^+}{\partial t} + \frac{\partial n_{im,m}^+}{\partial \tau} = -(l_{im,m}^+ + o_{im,m}) + r_m, \tag{14}$$

where the mobility fluxes are estimated by a bidirectional first-order kinetics under the assumption that 95% of ammonium are fixed to soil clay in an ideal equilibrium state between mobile and immobile ammonium (Porporato et al., 2003; Woo & Kumar, 2016; 2017).

We consider ammonia and mobile ammonium as a single species, indicated as mobile ammonia/ammonium, since these two species cannot be separated due to a dynamical equilibrium between ammonia and mobile ammonium. The gain of mobile ammonia/ammonium in the fracture ($n_{mo,f}$ [g·m^{-3}·day^{-1}]) arises from input from the surface ($e_{e,f}$ [g·m^{-3}·day^{-2}]) that includes fertilizer application and atmospheric deposition, mineralization (m_f [g·m^{-3}·day^{-2}]), and urea hydrolysis (h_f [g·m^{-3}·day^{-2}]). The loss terms of mobile ammonia/ammonium includes plant uptake (p_f^+ [g·m^{-3}·day^{-2}]), microbial uptake ($l_{mo,f}^+$ [g·m^{-3}·day^{-2}]), nitrification ($o_{mo,f}$ [g·m^{-3}·day^{-2}]), volatilization (v_f [g·m^{-3}·day^{-2}]), and loss through tile flow ($g_{mo,f}$ [g·m^{-3}·day^{-2}]). Here we also use the same gain and loss terms for the case of the matrix with subscript m instead of subscript f. By considering the divergence of advective mass flux, age flux, and the

ammonia/ammonium mass exchange flux between the fracture and matrix (Γ_n [g m^{-3} day^{-2}]), we get

$$\frac{\partial n_{mo,f}}{\partial t} + \frac{\partial n_{mo,f}}{\partial \tau} = \left(e_{e,f} + m_f + h_f\right) - (p_f^+ + l_{mo,f}^+ + o_{mo,f} + v + g_{mo,f}) - \frac{\xi_{im}^+}{\xi_{mo}^+} r_f - \Delta \cdot \left(\vec{u}_f \frac{n_{mo,f}}{\theta_f}\right) - \frac{\Gamma_n}{w_f} \tag{15}$$

and

$$\frac{\partial n_{mo,m}}{\partial t} + \frac{\partial n_{mo,m}}{\partial \tau} = \left(e_{e,m} + m_m + h_m\right) - (p_m^+ + l_{mo,m}^+ + o_{mo,m} + v + g_{mo,m}) - \frac{\xi_{im}^+}{\xi_{mo}^+} r_m - \Delta \cdot \left(\vec{u}_m \frac{n_{mo,m}}{\theta_m}\right) + \frac{\Gamma_n}{w_m}, \tag{16}$$

where

$$\Gamma_n = \Gamma_w \frac{n_{mo,w}}{\theta_w} + \frac{\beta}{a^2} D_{mo}(n_{mo,f} - n_{mo,m}) \tag{17}$$

and D_{mo} is an ammonia/ammonium diffusion coefficient (m^2/day). In case that the direction of water is from the matrix to the fracture: $n_{mo,w} = n_{mo,m}$ and $\theta_w = \theta_m$, and in the opposite case: $n_{mo,w} = n_{mo,f}$ and $\theta_w = \theta_f$.

By using equations (10) and (11), for example, the nitrate age of the bulk soil (a^- [day]) can be obtained as

$$a^-(t, \mathbf{x}) = \frac{w_f \int_0^\infty \tau n_f^-(t, \mathbf{x}, \tau) d\tau + w_m \int_0^\infty \tau n_m^-(t, \mathbf{x}, \tau) d\tau}{w_f \int_0^\infty n_f^-(t, \mathbf{x}, \tau) d\tau + w_m \int_0^\infty n_m^-(t, \mathbf{x}, \tau) d\tau}, \tag{18}$$

which is the mass-weighted average of the ages in the fracture and matrix.

It is noted that the birth and death events of nitrogen age are different from the gain and loss terms, respectively. The latter is associated with internal transformations, such as nitrification and mobility flux between immobile and mobile ammonia/ammonium. In other words, the inward fluxes from the outside of the control volume, such as nitrogen input from the surface, mineralization, and urea hydrolysis, are considered as the birth and/or age-zero events. The outward fluxes from the soil control volume, such as plant and microbial uptakes, volatilization, N_2O production by nitrification, denitrification, and volatilization, are considered as the death and/or age-loss events. The internal fluxes within the control volume, such as nitrification, mobility flux between immobile ammonium and mobile ammonia/ammonium, and flux exchange between the fracture and matrix, are considered as age conveyances. More details including nitrogen age equations and parameters are described in Woo et al. (2014) and Woo and Kumar (2016, 2017).

3.3. Tile Drainage Submodel

To capture the flow through the tile, we implement a tile flow model that is coupled to the spatially distributed 3-D ecohydrological and biogeochemical model. The movement of subsurface water to drainage pipes in a computational grid where tile drain is located is governed by soil hydraulic conductivity, soil water potential, spacing between tile drains, and tile drain depth (Green et al., 2006; Madramootoo & Broughton, 1987; Shen et al., 1998). Since tile flow occurs when the water potential of the soil exceeds that of tile drains (Arnold et al., 1999; Green et al., 2006), we use a parameter, tile flow trigger threshold (ψ_{tr}) following Green et al. (2006), to initiate tile flow under saturated conditions. The flow quantities from the fracture ($q_{T,f}$) and matrix ($q_{T,m}$) are estimated as

$$q_{T,f} = \begin{cases} K_p \frac{\psi_f - \psi_{tr}}{d_e}, & \text{if } \psi_f \geq \psi_{tr} \\ 0, & \text{otherwise} \end{cases} \tag{19}$$

and

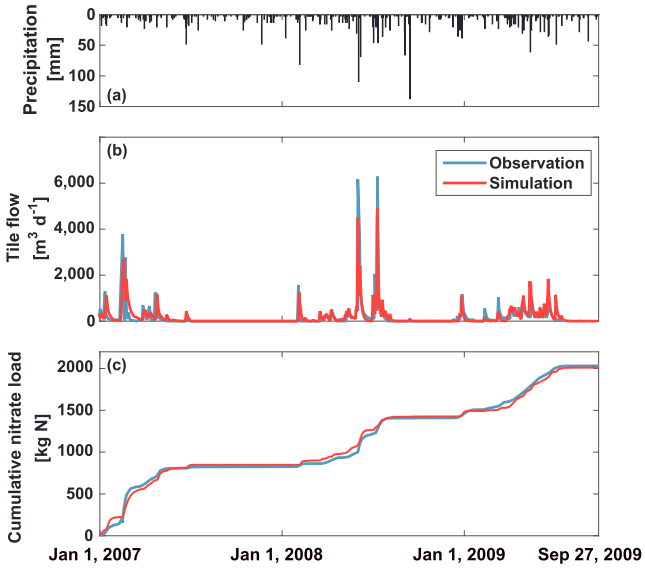

Figure 2. Comparison of modeled output with observations, (a) precipitation used as one of the drivers for the model, (b) tile flow at outlet of southern network (Figure 1), and (c) cumulative nitrate load in tile drainage flows from 1 January 2007 to 27 September 2009. The coefficients of determinations for tile flow and cumulative nitrate load are 0.60 and 0.99, respectively.

$$q_{T,m} = \begin{cases} K_p \frac{\psi_m - \psi_{tr}}{d_e}, & \text{if } \psi_m \geq \psi_{tr} \\ 0, & \text{otherwise,} \end{cases} \tag{20}$$

where K_p is tile drain hydraulic conductivity and d_e is effective drain spacing. The parameters K_p and d_e are obtained from previous work (Freeze & Cherry, 1979; Shen et al., 1998) and presented in Table 1.

Tile drain nitrogen loss is described by an advection equation that captures the transport of solutes. Nitrate and mobile ammonia/ammonium losses in tile drainage for the fracture and matrix are estimated using

$$g_f^- = q_{T,f} \frac{n_f^-}{\theta_f} \frac{1}{\Delta z}, \tag{21}$$

$$g_m^- = q_{T,m} \frac{n_m^-}{\theta_m} \frac{1}{\Delta z}, \tag{22}$$

$$g_{mo,f} = q_{T,f} \frac{n_{mo}}{\theta_f} \frac{1}{\Delta z}, \tag{23}$$

and

$$g_{mo,m} = q_{T,m} \frac{n_{mo}}{\theta_m} \frac{1}{\Delta z}, \tag{24}$$

where Δz is the height of soil vertical grid where tile drain is installed. Here n_f^-, for example, is divided by soil moisture (θ_f), so that the term, $\frac{n_f^-}{\theta_f}$, becomes nitrate concentration in the fracture per unit volume of soil water. Multiplying the terms by $q_{T,f}$ gives the nitrate loads of the fracture per unit surface area.

To reduce the boundary effects over the simulation domain, we used 20% buffer areas at all sides that are not used in the analysis of the impacts of subsurface tile drain systems on the concentration and age. At the surface lateral boundaries, free-flow boundary conditions are implemented while at the subsurface lateral boundaries, we use no-flow boundary conditions. For the bottom boundary condition, since the total soil depth used in this study is 1.6 m, it is unrealistic to define an impermeable bottom soil layer as generally used to simulate tile drainage systems (Buyuktas et al., 2004; Dusek et al., 2008; Gerke et al., 2007; Filipovic et al., 2014; Mohanty et al., 1997, 1998). We therefore used free flow at the bottom boundary with 0.1% of the saturated hydraulic conductivity of that used in the soil layers.

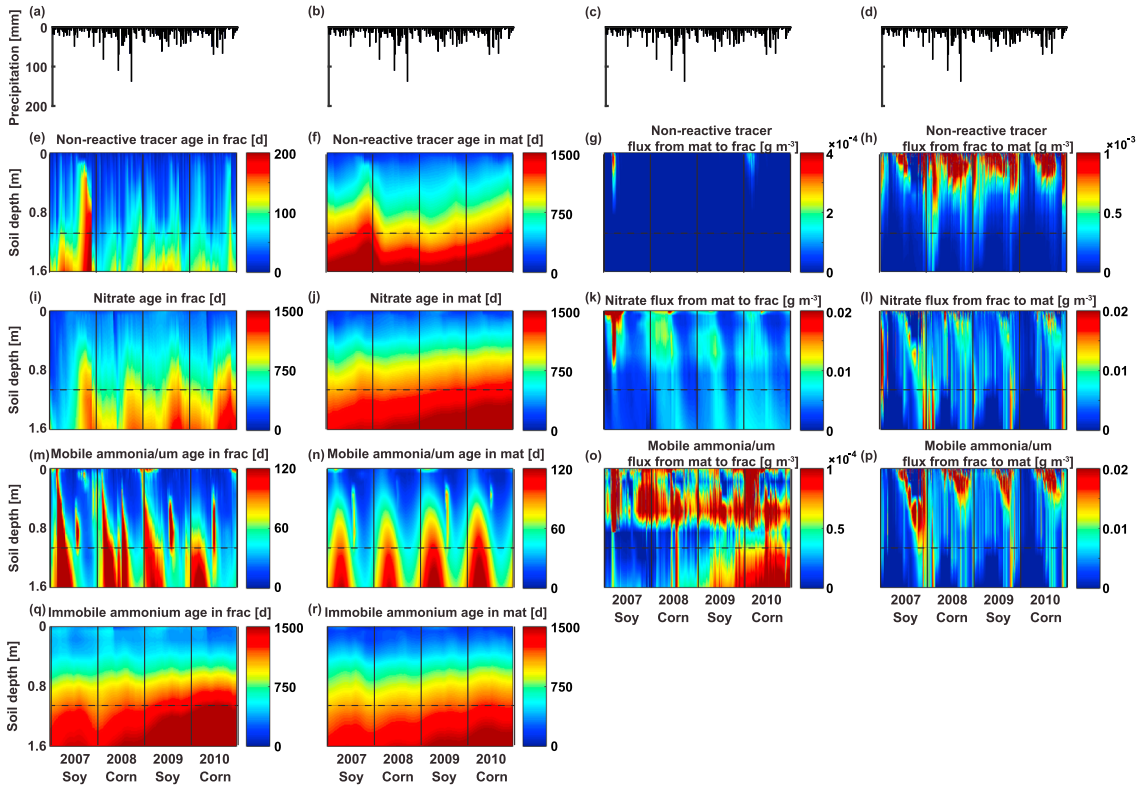

Figure 3. Illustration of age and flux dynamics in the soil column spatially averaged over the entire domain. (a), (b), (c), and (d) show the precipitation, which is the same and presented on top of each column to help visually see its influence on the ages of nonreactive tracer in the (e) fracture and (f) matrix; nitrate in the (i) fracture and (j) matrix; mobile ammonia/ammonium in the (m) fracture and (n) matrix; and immobile ammonium in the (q) fracture and (r) matrix. Also, nonreactive fluxes from the (g) matrix to the fracture and (h) fracture to matrix; nitrate fluxes from the (k) matrix to the fracture and (l) fracture to matrix; and mobile ammonia/ammonium fluxes from the (o) matrix to fracture and (p) fracture to matrix are illustrated to explore the age conveyances between the fracture and matrix.

4. Results

4.1. Model Validation

As a first step, we compare the model response with observed data available for tile flow from a previous study (Woli et al., 2010). We conduct the comparisons of results obtained from the simulations of the 3-D coupled ecohydrological-biogeochemical model against the observations of flow and nitrogen loads in the southern tile drainage over 3 years (Figure 2). The results agree well with published experimental data. However, the performance of tile flow is somewhat muted during relatively high peak flows that inevitably has an effect on the accuracy of the nitrogen loads. The mismatch of the flows and nitrate loads is in part due to the precipitation data used in the simulation, which are not collected at the study site but from a weather station ~40 km away. However, the tile flow and nitrate loads generally capture the patterns of the observed data, which were primarily due to the implementation of the dual-permeability model (see Appendix for the detailed analysis of the model). These agreements provide confidence in the use of the simulation results for broader understanding described below. At this time there is no direct way to validate the age distribution of nitrogen, so it remains a model inferred quantity.

4.2. Age of Nitrogen in Fracture and Matrix

Figure 3 shows the ages of nonreactive tracer, nitrate, mobile ammonia/ammonium, and immobile ammonia or ammonium in the fracture and matrix to the depth of 1.6 m, which are spatially averaged over the entire domain. As expected, their ages in the fracture penetrate readily into deeper soil layers compared to those in the matrix due to low bulk density and high saturated hydraulic conductivity. This results in younger ages deeper into the vertical column in the fracture as compared to the matrix. This demonstrates the extent to which preferential flow paths allow the rapid transport of nonreactive tracer and inorganic nitrogen from the upper soil layers to the deeper zones along with high water infiltration during precipitation events. It is noted that the mass exchange flux between fracture and matrix is dominant in the direction

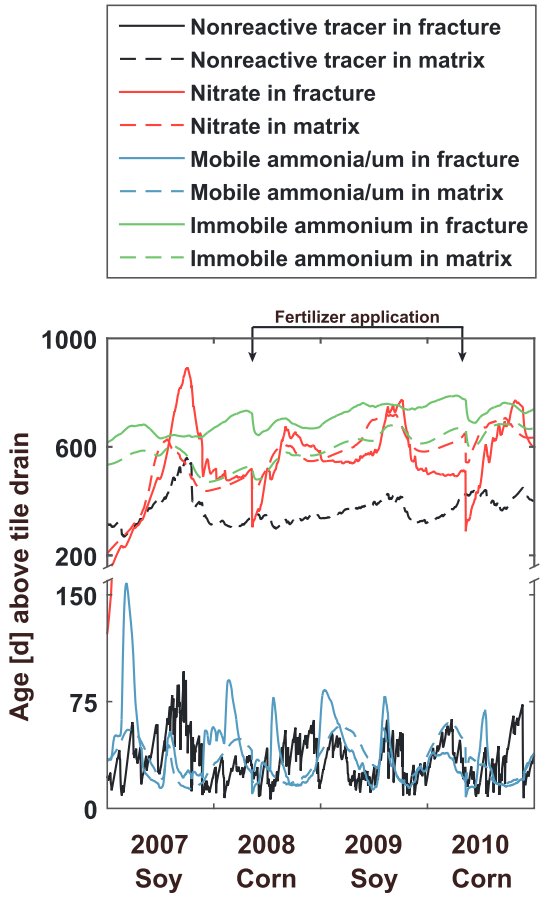

Figure 4. Column-based and mass-weighted averages of the age of nonreactive tracer and inorganic nitrogen species considered above tile drains (to the depth of 1.2 m) in the fracture (solid line) and the matrix (dashed line) are presented.

from fracture to matrix, which results in the retardation of the chemical constituents as it moves through the matrix. It is thus observed that the age of nonreactive tracer in the fracture is much lower than that in the matrix. However, the difference in the age of nitrate between the fracture and the matrix is not distinct and even higher in the matrix during nontile flow periods. This is because of nitrification that is associated with the age conveyance of nitrogen from ammonium to nitrate. The reduced concentration in mobile ammonia/ammonium in the fracture due to the fast transport paths increases the mobility flux from immobile ammonium to mobile ammonia/ammonium, thus increasing the age of the latter. The increased ages of ammonium in turn increase the age of nitrate in the fracture through nitrification.

Figure 4 shows the column-based and mass-weighted averages of the age of nonreactive tracer, nitrate, mobile ammonia/ammonium, and immobile ammonium in the fracture and matrix above tile drains (to the depth of 1.2 m) over the study period. The age of nonreactive tracer in the fracture is much lower than that in the matrix. The ages of mobile ammonia/ammonium in the fracture and matrix are lower than those of the other nitrogen species since mobile ammonia/ammonium regularly obtains more nitrogen with age zero through mineralization and fertilizer application. The age of immobile ammonium in the fracture is constantly higher than that in the matrix over the study period. The rapid transport of mobile ammonia/ammonium in the fracture to deeper soil layers triggers a strong increase in the flux from immobile ammonium to mobile ammonia/ammonium and thus decrease the flux in the opposite direction.

4.3. Impacts of Tile Drainage on Age Distribution

Figure 5 shows the differences between simulations with and without the tile drainage submodel for the concentrations of nonreactive tracer, nitrate, immobile ammonium, and mobile ammonia/ammonium, and their ages that are spatially averaged over the subsurface domain (with tile drain minus without tile drain). To explore the effects of the tile drain on soil nitrogen concentration and its age, other parameters and forcings are maintained identical. Here we also show the concentration and age of nonreactive tracer for comparison.

The drainage system significantly reduces the concentrations of nonreactive tracer, nitrate, immobile ammonium, and mobile ammonia/ammonium in the soil, especially during the period when tile drainage occurs (not shown). However, we observe occasional, but noticeable, increases in the inorganic soil nitrogen concentration in the topsoil layers compared to the case without the tile drain submodel. The decreased soil moisture due to the removal of excess soil water results in increased infiltration and soil temperature by suppressing latent heat flux. These hydrologic responses due to tile drainage create a favorable condition for aerobic microbial processes, such as mineralization and nitrification. We also observe increased concentrations of nonreactive tracer, nitrate, immobile ammonium, and mobile ammonia/ammonium below the tile drains. Less wet soils due to the removal of soil water compared to the nontile drainage cases result in a decrease in the downward fluxes of water below the tile drains. These dynamics reduce the loss of nonreactive tracer and nitrogen to the deeper soil layers below the tile line.

There is a general agreement that tile drains shorten the time elapsed between the influx of water and nutrient, and outflux through rapid transport (e.g., Randall & Mulla, 2001 and Van Meter & Basu, 2017). In general, our results are consistent with this common knowledge, especially for the nonreactive tracer, nitrate, and immobile ammonium above the tile drains. However, below the tile drains, we observe increases in the age of nonreactive tracer and nitrogen. This arises due to the reduced migration of nonreactive tracer and nitrogen beyond the tile drains, leading to a lower chance of mixing with younger chemical constituents. In addition, unlike the case of nonreactive tracer, increased age of inorganic soil nitrogen is

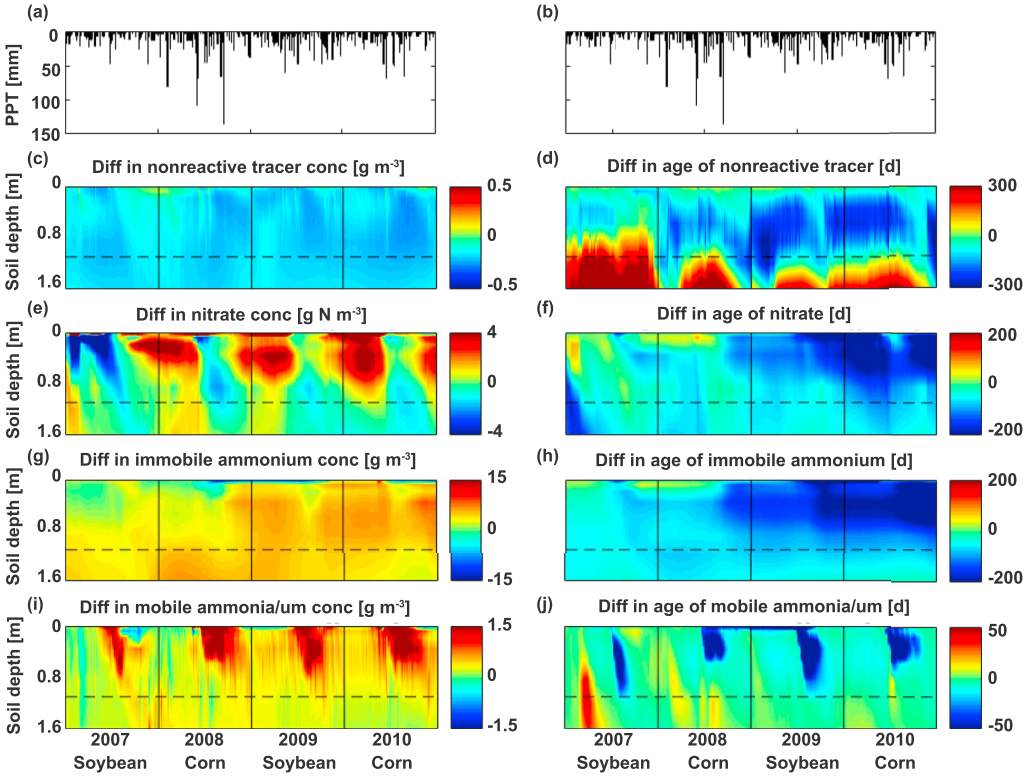

Figure 5. Illustration of the impact of tile drainage on the vertical concentration and age distribution. (a) and (b) show the precipitation the same for each column. The differences between with and without the tile drainage submodel over the study period (with tiles minus without tiles) for (c) nonreactive tracer concentration, (d) age of nonreactive tracer, (e) nitrate concentration, (f) age of nitrate, (g) immobile ammonium concentration, (h) age of immobile ammonium, (i) mobile ammonia/ammonium concentration, and (j) age of mobile ammonia/ammonium. The black dashed line represents the location of the tile drain.

observed above the tile drains. Nitrification triggers a transformation-dependent increase in the age of nitrate that is associated with both increased ages of immobile ammonium and mobile ammonia/ammonium.

4.4. Influence of Topographic Variability on Age of Nitrogen

Figure 6 shows soil moisture, nitrate concentration, and its age averaged over the study period for the bulk soil to the depth of 1.6 m across the West-East transect (white dashed line in Figure 1). Decreases in soil moisture and nitrate concentration above the tile drain are observed (Figures 6a and 6b). The subsurface water flow due to tile drainage removes nitrate from the soil above the tile drain. On the other hand, decreases and increases in the age of nitrate are observed in the soil above and below the tile drains, respectively (Figure 6c). Topsoil usually obtains younger nitrate constituents more than the other layers through fertilizers, and atmospheric deposition. The lower age of nitrate above the tile drains indicates that tile drain system reduces the length of time spent by nitrate in the soil by increasing the efflux of nitrate through subsurface tile drainage.

To understand the spatial distribution of nitrate and its age above and below tile drains, their column averaged values over the study period are shown in Figure 7. We use the 5th and 95th percentile values of the given probability distributions to effectively visualize the effects of tile drainage. The results show that there is significant variation in soil nitrate and its age across the study site, which is strongly related to topographic depressions and subsurface tile drain system. The topographic depressions are persistently associated with low nitrate concentrations even in the areas where the tile drains are located. The relatively higher surface water storage in depressions increases the vertical moisture flux. This higher water flux transports a larger amount of dissolved inorganic nitrogen to the deeper soil layers (Woo & Kumar, 2017). The drainage tile, of course, decreases soil moisture and, therefore, amplifies the potential for nitrate losses through tile flows.

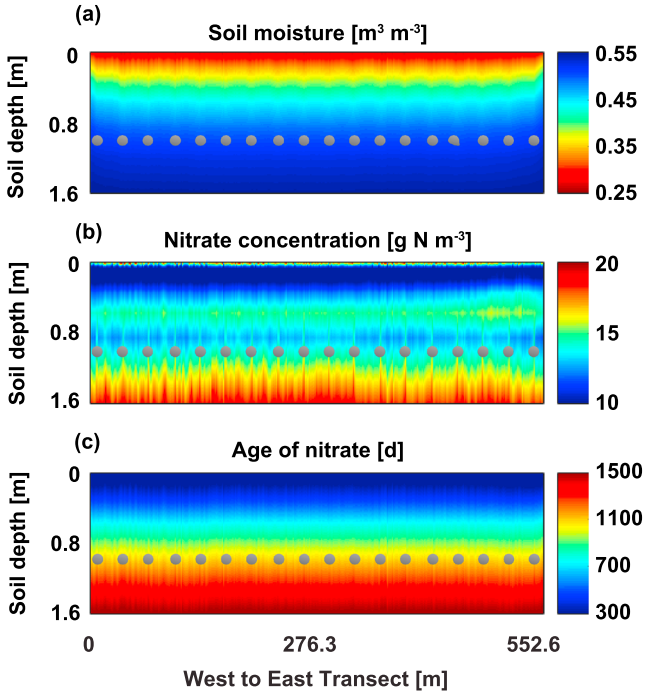

Figure 6. Profile of (a) soil moisture, (b) nitrate concentration, and (c) its age across the West-East transect as indicated in Figure 1, which are averaged over the study period of 2007 to 2010. The gray dots represent the tile drains at a depth of 1.2 m.

The age of nitrate clearly delineates the position of tiles by providing the cumulative history of the transformation and transport of soil nitrate dynamics (Figure 7e). The conveyance of age from ammonium to nitrate through nitrification increases the age of nitrate in areas where tile drains are installed more than that in the adjacent areas. Also, the travel time of nitrate increases its age due to flow convergence toward tile drain inlets. These processes shape the spatial distribution of nitrate age.

4.5. Combined Age-Concentration Analysis

The age and concentration can be analyzed together to provide further insights. To conduct this combined analysis, Figure 8 shows the joint probability distribution functions above tile drains averaged over the study period. The intersection points of the 50th percentiles of the marginal distributions are used to define the high and low categorization of both concentration and age. This coupled analysis allows us characterize the spatial variability of dominant processes. When the age of nitrate is low and the concentration is high (Figure 8a), it indicates that nitrate fertilizer application and atmospheric nitrate deposition are the dominant processes since they are assumed as birth processes providing younger molecules in the control volume. The dominant nitrate loss process, which includes crop and microbial nitrate uptakes and denitrification, drives a decrease in nitrate concentration, but an increase in nitrate age with time. The presence of both low age and concentration indicates that nitrate efflux is the dominant process since dissolved nitrate moves downward, thus removing the older nitrate present in the near-surface layers. In contrast, low efflux of nitrate and high nitrification drive an increase in both nitrate age and concentration since nitrification is driven by ammonium that is at a higher age than that of nitrate due to the cation exchange of ammonium with the clay mineral. In areas far from tile drains, we observe relatively higher age and lower concentration of nitrate above tile drains (Figure 8b).

For the case of immobile ammonium (Figure 8c), when both age and concentration are high, it indicates that the dominant process in the soil is the loss of immobile ammonium, which includes microbial uptake, nitrification, and mobility flux to mobile ammonia/ammonium. There is an order of magnitude difference between the age of immobile ammonium and that of mobile ammonia/ammonium. Therefore, the mobility flux from mobile ammonia ammonium will decrease the age of immobile ammonium regardless of the flux magnitude. In the areas above tile drains, low age and varied concentration of immobile ammonium are observed (Figure 8d). During tile flow, the removal of mobile ammonia/ammonium occurs, consequently

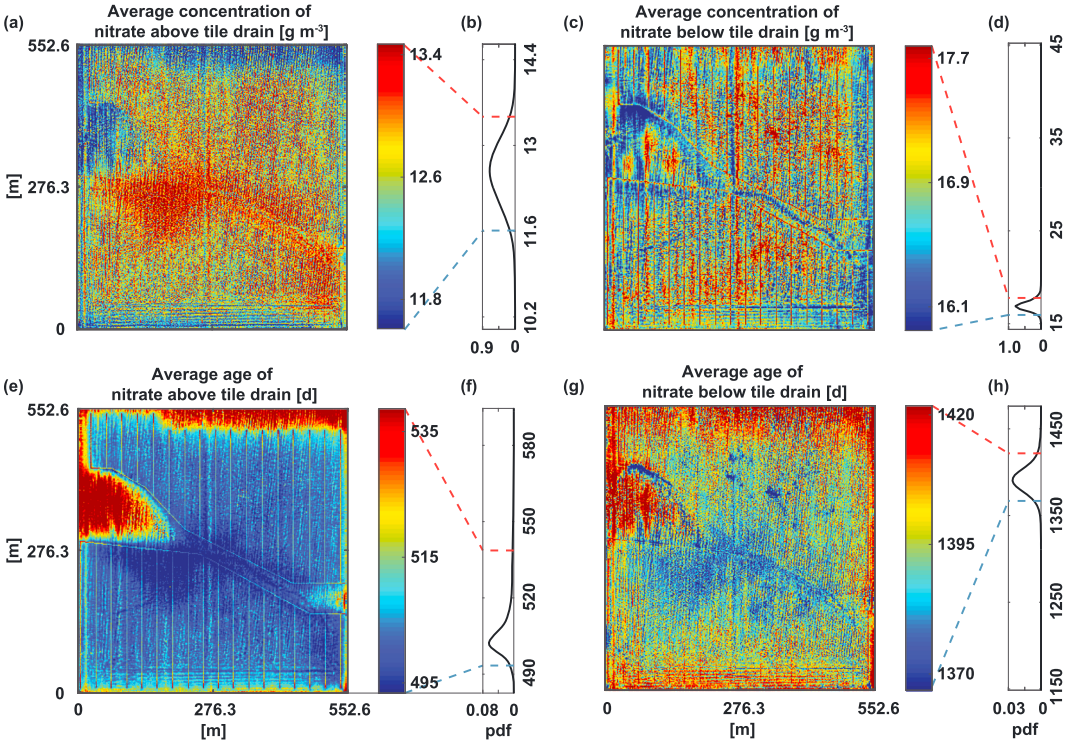

Figure 7. Illustration of the spatial distribution of nitrate concentration (top row) and age (bottom row) above (left column) and below (right column) the tile system. Column averaged (a and c) nitrate concentrations and (b and d) their probability distribution functions (pdf) above and below the tile drains over the study period, respectively. (e and g) Mass-weighted averages of the ages of nitrate and (f and h) their pdfs above and below the tile drains, respectively. The blue and red dashed lines represent the corresponding 5th and 95th percentiles of the given pdfs, respectively.

increasing the mobility flux from immobile ammonium to mobile ammonia/ammonium. At the same time, due to the removal of excess water that creates favorable conditions for mineralization, increased amount of mobile ammonia/ammonium are turned into immobile ammonium. During the periods when tile drainage does not occur, the relatively young age of mobile ammonia/ammonium mixes with the relatively old age of immobile ammonium, thus decreasing the age of the latter above tile drains. Below tile drains, in general, low immobile ammonium age and high immobile ammonium concentration are observed (not shown), indicating that the dominant process is the mobility flux from mobile ammonia/ammonium to immobile ammonium. It is noted that the areas that are classified as topographic depressions have high age and low concentration of immobile ammonium. Due to the consistent downward movement of water that also carries dissolved mobile ammonia/ammonium to the deeper soil layers in these areas, the relatively higher mobility flux from immobile ammonium to mobile ammonia/ammonium constantly occurs. This process in turn reduces the mobility flux from mobile ammonia/ammonium to immobile ammonium, thus increasing the age of the latter.

For the case of mobile ammonia/ammonium (Figure 8e), when its age and concentration are low, it indicates that the birth of mobile ammonia/ammonium is the dominant process, which includes fertilizer application, atmospheric deposition, and mineralization. The dominant loss process, which include crop and microbial uptakes, nitrification, volatilization, and mobility flux to immobile ammonium, will decrease its concentration but increase its age over time. High efflux will decrease its concentration, but increase age, and vice versa. Due to the significant difference between the age of immobile ammonium and that of mobile ammonia/ammonium, the mobility flux from immobile ammonium to mobile ammonia/ammonium will increase the age of the latter independent of the amount of mobility flux. It is noted that the areas above tile drains have both high age and low concentration of mobile ammonia/ammonium (Figure 8f). As indicated, due to the high movement of water to tile drains, which also carries mobile ammonia/ammonium, the high mobility flux from immobile ammonium to mobile ammonia/ammonium occurs during tile flow

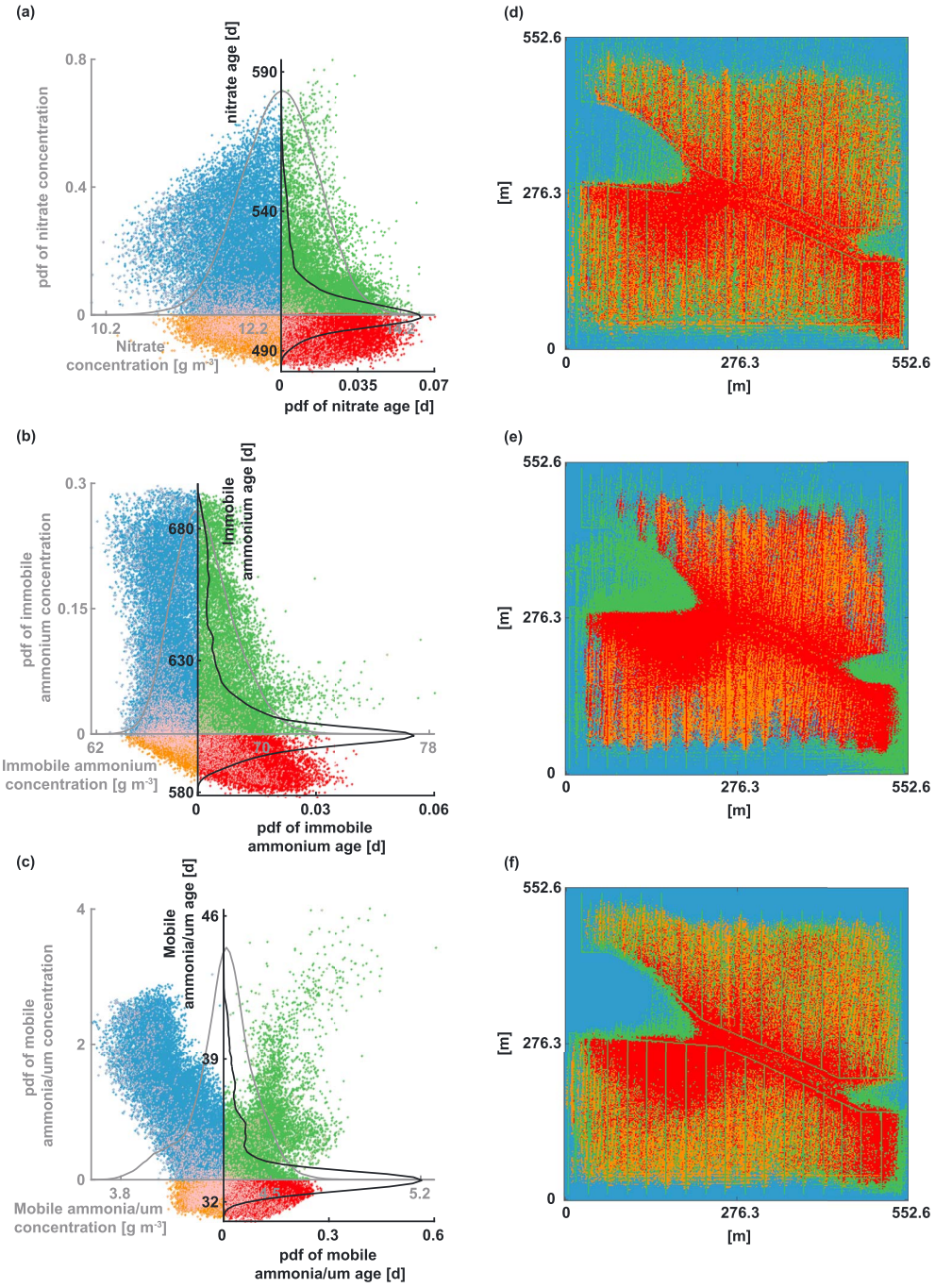

Figure 8. Illustration of the joint variability of column averaged concentration and age above the tile drains. Each plot in the left column shows the probability distribution function of concentration (solid gray curve) and age (solid black curve) along two orthogonal axes that are placed at the intersection of their respective median. The four sections in different colors therefore represent the combinations of high and low concentrations and ages for (a) nitrate, (b) immobile ammonium, and (c) mobile ammonia/ammonium. Each point in a plot represents a specific spatial grid and is mapped to the spatial domain (right column) to explore the corresponding spatial characteristics for (d) nitrate, (e) immobile ammonium, and (f) mobile ammonia/ammonium, respectively. The pink dots in (a), (b), and (c) represent the areas where topographic depressions are present.

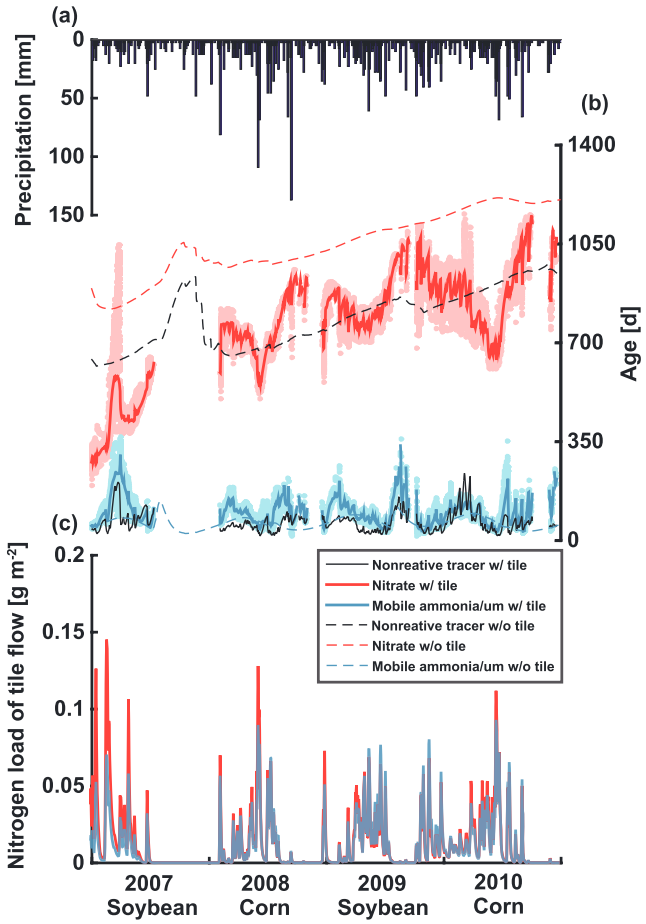

Figure 9. Illustration of the variation of age and concentration through the tile system outlet. (a) Precipitation. (b) Mass-weighted age of nonreactive tracer (solid black line), nitrate (solid red line), and mobile ammonia/ammonium (solid blue line) are overlaid on the ensemble of the given ages in tile drainage. For the purpose of comparison, we also show the mass-weighted age of nonreactive tracer (dashed black line), nitrate (dashed red line), and mobile ammonia/ammonium (dashed blue line) in the soil, which are obtained in the simulations without the subsurface tile drain model. (c) Nitrate and mobile ammonia/ammonium loads in tile drainage over the study period.

events. This process increases the age and concentration of mobile ammonium. In this way, the combined analysis of the age and concentration of inorganic nitrogen species provides insights into the spatial distribution of dominant processes, which is beyond what can be obtained by analyzing inorganic nitrogen concentration only.

4.6. Age Distribution in Tile Flow

How long do nonreactive tracer and inorganic nitrogen stay in the soil before entering the stream? Toward this question, we study (Figure 9) the age of nonreactive tracer, nitrate, and mobile ammonia/ammonium along with their loads in the efflux from tile drainage. The age of nonreactive tracer in tile drainage is younger than 1 year in the study site. The age of nitrate in tile drainage ranges from 1 to 3 years while that of mobile ammonium are between a few days and a year. Nitrification is one of the major sources of nitrate even in agricultural fields next to fertilizer application, which requires the transformation of ammonium to nitrate. However, for mobile ammonia/ammonium, an increase in age is observed due to the nitrogen transformation between immobile ammonium and mobile ammonia/ammonium. The significant amount of mobile ammonia/ammonium transported to tile drains results in release of immobile ammonium, with relatively high age due to its fixation by clay minerals, to mobile ammonia. Because of this, we observe an unexpected increased age of mobile ammonia/ammonium under the presence of tile drains.

5. Summary and Discussion

Three-dimensional numerical simulations have been performed to explore the impacts of subsurface tile drains on the distribution of inorganic soil nitrogen ages and concentrations and compared to that of nonreactive tracer. We expanded the *Dhara* model (Le & Kumar, 2017; Woo & Kumar, 2017) to include dual-permeability and subsurface tile drain models. The use of mean age theory applied to inorganic soil nitrogen allows for a unique understanding of the impacts of tile drains by exploring its timescale components. We find that the age of inorganic soil nitrogen in the fracture is not always lower than that in the matrix. Also, our results show that in topographic depressions, both the concentration and age of nitrate are lower than elsewhere even with tile drain systems, indicating their important roles in determining the heterogeneity of soil nitrogen dynamics. Through the combined analysis of nitrate concentration and age, the high concentration and low age are observed in the areas near the tile drains. While previous studies (e.g., Arnold et al., 1999; Ernstsen et al., 2015; Green et al., 2006; Lavaire et al., 2017) have focused on understanding the impacts of tile drains on inorganic nitrogen concentration only, this study is the first attempt to explore and analyze their impacts on the concentration and age together.

In recent decades, a number of studies (Arora et al., 2012; Beven & Germann, 2013; Bishop et al., 2015; Cuthbert et al., 2013; Ford et al., 2017; Kohne et al., 2002; Nimmo, 2012; Simunek & van Genuchten, 2008) have demonstrated that water flow and nutrient transport in the unsaturated zone is greatly influenced by preferential flow paths. Consistent with these previous findings, the inclusion of macropore flow into *Dhara* significantly increases its ability to predict subsurface nitrogen losses. However, in contrast to the common knowledge of residence time and age in the fracture, the age of inorganic nitrogen in the fracture is not always lower than that in the matrix. In particular, for the case of immobile ammonium, its age in the fracture is consistently higher than that in the matrix over the 4-year study period. The relatively high age in the fracture is primarily due to cation exchange between ammonium and clay minerals, which is important in influencing the retention of inorganic nitrogen in the soil. This result indicates that if reactive tracers,

nitrogen in this study, were to be considered as nonreactive tracers by ignoring reaction dynamics, their ages would be underestimated and would result in misleading conclusions.

There has been a growing interest in estimating the age of chemical constituents in the field of hydrology using residence time distributions (RTDs) and transit time distributions (TTDs) (e.g., Botter et al., 2011; Cvetkovic, 2011; Dagan, 1989; Harman & Kim, 2014; Rinaldo et al., 2011). Differently from what was explored by using RTDs and TTDs, we applied the general theory of mean age to the case of inorganic soil nitrogen based on (Woo & Kumar, 2016, 2017), which in turn were based on Danckwerts, (1953, 1958), Ginn, (1999, 2000), and Deleersnijder et al. (2001). The estimation of nitrogen age requires consideration of periodic fertilizer application and nitrogen transformation processes in responses to weather variability. The temporal and spatial patterns of soil inorganic nitrogen age estimated in this study can thus provide dynamical attributes not captured by RTDs that estimate a spatially integrated age spectrum under a quasi steady state assumption (Zhang et al., 2010) nor by TTDs that are insufficient for nonlinear transient dynamics (Ginn, 1999; Kim et al., 2016; Luo & Cirpka, 2011).

Nitrogen fertilizer application is one of the essential factors required to improve productivity in agriculture (e.g., Ayub et al., 2002; Kogbe & Adediran, 2003). However, only half of nitrogen applied is absorbed by crops (Gardner & Drinkwater, 2009), which indicates that the other half accumulates in the soil or leaches to receiving water bodies. In fact, these transport processes are accelerated under tile-drained agricultural fields by providing faster flow routes. In addition, Richardson and Kumar (2017) find that 50% of energy consumption in agricultural practices is from the use of nitrogen fertilizer. To make these practices sustainable, a field-based precision nitrogen fertilizer application can provide a strategy to protect the environment and reduce energy consumption (Van Alphen & Stoorvogel, 2001). The spatial distribution of concentration and age of nitrogen presented in this study can provide new insights into the precision management for enhancing fertilizer use efficiency. The relatively high concentration and low age of nitrate are observed in the areas near tile drains (dominant birth process), and the low concentration and high age of nitrate are observed in the areas relatively far from tile drains (dominant loss process) as shown in Figure 7. These findings indicate split fertilizer strategies can be used to effectively reduce the nitrogen load entering surface waters: a decrease in nitrogen fertilizer rates in the areas near tile drains and an increase in its rates in the other areas.

This study also opens the need to develop methods for the validation of age distribution in the soil and tile drain efflux. The use of stable isotopes of nitrogen might be an option to trace the transport and fate of nitrogen (e.g., Bedard-Haughn et al., 2003). However, while establishing a direct relationship between the simulated age and observed isotopic variability from tile-based measurement can help validate the age model, at this time such methods are not available. We hope that this study motivates future research that focuses on exploring novel experimental and analytical procedures toward this goal. In addition, the inability of the model to capture the peak flows could be attributed to the preferential flow method used in this study. Stone and Wilson (2006) found that preferential flow accounts for up to 80% of peak flow in tile drainage by using chloride as a tracer in an agricultural field. However, incorporating the actual paths of preferential flow into a model requires the characterization of its paths (Mohanty et al., 1998) or the direct observation that is often difficult to be measured at a field scale (Abou Najm et al., 2010). Therefore, in this study, due to another level of uncertainty for the assumption and lack of measured data, the preferential flow dynamics are developed by implementing a dual-permeability approach with a fixed matrix or fracture fraction. However, our work allows for a more complete assessment of inorganic soil nitrogen dynamics, as this would improve our understanding of the spatial and temporal distribution of inorganic nitrogen concentration and age in relevance with tile drain systems.

Appendix

The tile water discharge estimated by the matrix flow only is compared to that estimated by the two mobile interacting pore domains developed in this study as shown in Figure A1. The tile flow peaks in response to precipitation are not accurately captured by the simulations of the matrix flow only, indicating an important role in preferential flow paths in the movement of soil water. To determine and explore the impacts of the volumetric fractions of the fracture and matrix on tile flow, the different volumetric fractions of fracture regions (15%, 20%, and 25%) are used to compare their performances. The results show that in general as the fracture region increases, tile peak flow becomes higher, but the duration of tile flow decreases (Figure A1b).

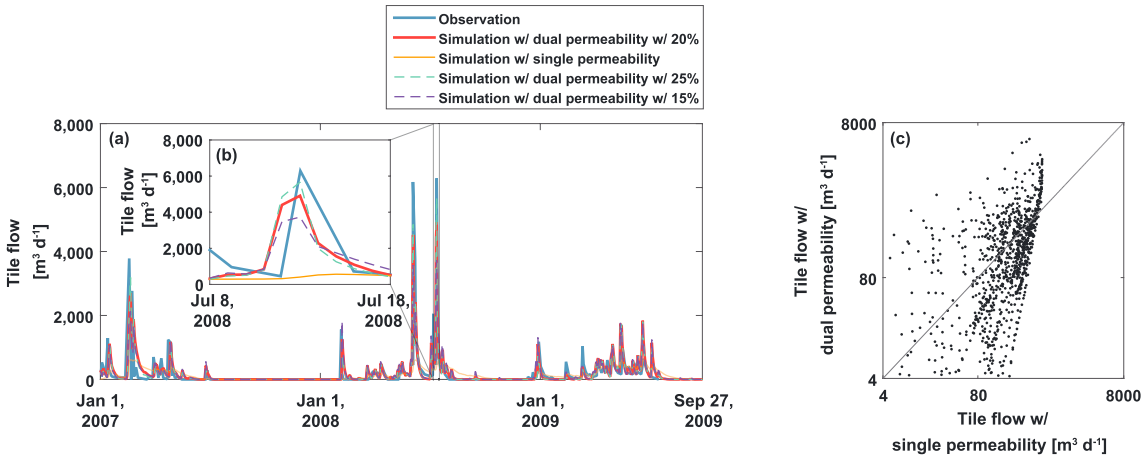

Figure A1. Illustration of the effect of fracture fraction in the dual-permeability model. Comparisons between observed and simulated tile flow at the outlet of the southern tile network under different scenarios. (b) depicts a zoomed-in period of (a). We compare the performances of dual-permeability medium ($w_m = 0.8$) with matrix permeability only ($w_m = 1$). To explore the dynamics related to the amount of fracture structures, we also compare the performance of tile flow under the different volumetric fractions ($w_f = 0.15$, 0.2, and 0.25). The blue and red lines are observation and simulation, respectively, used in the analysis of the impacts of tile drains on the age and concentration of inorganic soil nitrogen in this study and are the same as shown in Figure 2. The gray line in (c) represents the 1:1 relationships.

Field management data including fertilizer application before 2007 are not available, and thus, we conduct the model spinup following recorded management practices from 2007 to 2009 in the study site (Woli et al., 2010). However, at the beginning of the simulation period, the underestimation of nitrate load in tile-drained water is observed as shown in Figure A2. To address this discrepancy, the assumption of 24 g·N·m^{-2} of nitrate fertilizer applied during autumn 2006 is explored. This practice improves its predictions, which showed, especially, better match in the beginning in 2007 than the simulation without the assumption. Also, the impacts of different volumetric fractions of fracture regions (15%, 20%, and 25%) on nitrate loss through tile drainage are examined. The loss under the assumption of 25% fracture is higher than those under the lower amounts of the fractures compared in this study.

Based on the performances of tile flow and nitrate load explored, we find that results obtained with (1) 20% fracture and (2) 24 g·N·m^{-2} of nitrate fertilizer applied during autumn 2006 provide better matches with the observations than the others, and thus, we use them for our analysis.

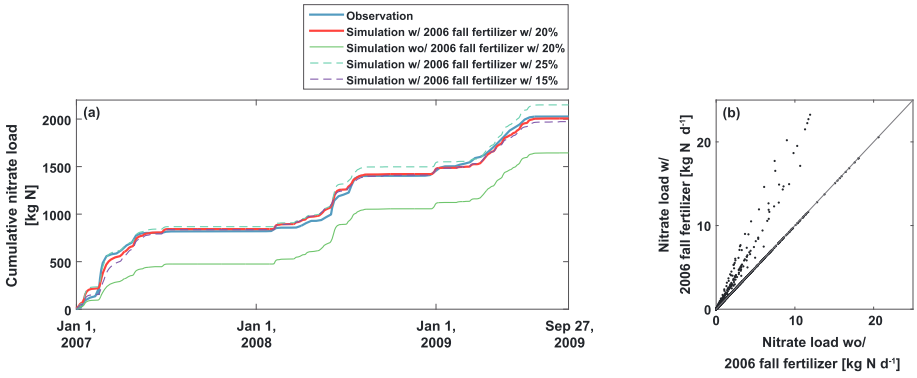

Figure A2. Illustration of the effect of nitrate fertilizer application on nitrate loss through tile drainage. Comparisons between observed and simulated cumulative nitrate load at the outlet of the southern tile network under different scenarios. We assess the assumption of 24 g·N·m^{-2} of nitrate fertilizer applied at autumn 2006. To explore the dynamics related to the amount of fracture structures, we also compare the performance of nitrate loss under the different volumetric fractions ($w_f = 0.15$, 0.2, and 0.25). The blue and red lines are observation and simulation, respectively, used in the analysis of the impacts of tile drains on the age and concentration of inorganic soil nitrogen in this study and are the same as shown in Figure 2. The gray line in (b) represents the 1:1 relationships.

Acknowledgments
We thank Hari Rajaram for discussions that led to the implementation of the dual-permeability model. This work was supported by the National Science Foundation (NSF) Grants CBET 1209402, ACI 1261582, EAR 1331906, and EAR 1417444. All of the numerical information in the figures is produced by solving the equations in the paper. The weather data are obtained from National Solar Radiation Data Base (http://rredc.nrel.gov/solar/old_data/nsrdb) and National Oceanic and Atmospheric Administration (https://www.ncdc.noaa.gov/cdo-web/datasets). LiDAR digital elevation data are obtained from Illinois State Geological Survey (http://clearinghouse.isgs.illinois.edu/data).

References

Abou Najm, M. R., Jabro, J. D., Iversen, W. M., Mohtar, R. H., & Evans, R. G. (2010). New method for the characterization of three-dimensional preferential flow paths in the field. *Water Resources Research*, *46*, W02503. https://doi.org/10.1029/2009WR008594

Arnold, J. G., Srinivasan, R., Ramanarayanan, T. S., & Diluzio, M. (1999). Water resources of the Texas Gulf Basin. *Water Science & Technology*, *39*(3), 121–133. https://doi.org/10.1016/S0273-1223(99)00224-3

Arora, B., Mohanty, B. P., & McGuire, J. T. (2012). Uncertainty in dual permeability model parameters for structured soils. *Water Resources Research*, *48*, W01524. https://doi.org/10.1029/2011WR010500

Ayub, M., Nadeem, M. A., Sharar, M., & Mahmood, N. (2002). Response of maize (Zea mays l.) fodder to different levels of nitrogen and phosphorus. *Asian Journal of Plant Sciences*, *1*, 352–354. https://doi.org/10.3923/ajps.2002.352.354

Bedard-Haughn, A., van Groenigen, J. W., & van Kessel, C. (2003). Tracing ^{15}N through landscapes: Potential uses and precautions. *Journal of Hydrology*, *272*, 175–190. https://doi.org/10.1016/S0022-1694(02)00263-9

Beven, K., & Germann, P. (2013). Macropores and water flow in soils revisited. *Water Resources Philosophy and Phenomenological Research*, *49*, 3071–3092.

Bishop, J. M., Callaghan, M. V., Cey, E. E., & Bentley, L. R. (2015). Measurement and simulation of subsurface tracer migration to tile drains in low permeability, macroporous soil. *Water Resources Philosophy and Phenomenological Research*, *51*, 3956–3981.

Bolin, N., & Rodhe, H. (1973). A note on the concepts of age distribution and transit time in natural reservoirs. *Tellus*, *25*, 58–62. https://doi.org/10.1111/j.2153-3490.1973.tb01594.x

Botter, G., Bertuzzo, E., & Rinaldo, A. (2011). Catchment residence and travel time distribution: The master equation. *Geophysical Research Letter*, *38*, L11403. https://doi.org/10.1029/2011GL047666

Buyuktas, D., Wallender, W., Soppe, R., Ayars, J., & Sivakumar, B. (2004). Calibration and validation of a three-dimensional subsurface irrigation hydrology model. *Irrigation and Drainage Systems*, *18*(3), 211–225.

Canter, L. W. (1997). *Nitrates in groundwater*. Florida USA: Lewis Boca Raton.

Chen, X., Pan, G., & Shen, Q. (2001). The vertical transport of solute rule in the agricultural land of Taihu area. *Chinese Environment Science*, *21*, 481.

Cuthbert, M. O., Mackay, R., & Nimmo, J. R. (2013). Linking soil moisture balance and source-responsive models to estimate diffuse and preferential components of groundwater recharge. *Hydrology and Earth System Sciences*, *17*, 1003–1019. https://doi.org/10.5194/hess-17-1003-2013

Cvetkovic, V. (2011). The tempered one-sided stable density: A universal model for hydrological transport? *Environ, Research Letters*, *6*(3), 034008. https://doi.org/10.1088/1748-9326/6/3/034008

Dagan, G. (1989). *Flow and transport in porous formations*. N. Y: Springer.

Danckwerts, P. (1953). Continuous flow systems: Distribution of residence times. *Chemical Engineering Science*, *2*, 1–13. https://doi.org/10.1016/0009-2509(96)81810-0

Danckwerts, P. (1958). The effect of incomplete mixing on homogeneous reactions. *Chemical Engineering Science*, *8*, 93–102. https://doi.org/10.1016/00092509(58)80040-8

de la Cretaz, A. L., & Barten, P. K. (2007). *Land use effects on streamflow and water quality in the Northeastern United States*. Boca Raton: CRC Press. https://doi.org/10.1201/9781420008722

Deleersnijder, E., Campin, J., & Delhez, E. J. M. (2001). The concept of age in marine modelling I. Theory and preliminary model results. *Journal of Marine Systems*, *28*, 229–267. https://doi.org/10.1016/S0924-7963(01)00026-4

Delhez, E. J., Lacroix, G., & Deleersnijder, E. (2004). The age as a diagnostic of the dynamics of marine ecosystem models. *Ocean Dynamics*, *54*, 221–231. https://doi.org/10.1007/s10236-003-0075-2

Dinnes, D. L., Karlen, D. L., Jaynes, D. B., Kaspar, T. C., Hatfield, J. L., Colvin, T. S., & Cambardella, C. A. (2002). Review and interpretation: Nitrogen management stategies to reduce nitrate leaching in tile-drained midwestern soils. *Agronomy Journal*, *153*, 153–171.

Du, B., Arnold, J. G., Saleh, A., & Jaynes, D. B. (2005). Development and application of swat to landscapes with tiles and potholes. *Transactions American Society of Association Executives*, *48*(3), 1121–1133.

Duffy, C. (2010). Dynamical modeling of concentration-age-discharge in watersheds. *Hydrological processes*, *24*, 1711–1718. https://doi.org/10.1002/hyp.7691

Dusek, J., Gerke, H. H., & Voge, T. (2008). Surface boundary condions in two-dimensional dual-permeability modeling of tile drain bromide leaching. *Vadose Zone Journal*, *7*(4), 1287–1301. https://doi.org/10.2136/vzj2007.0175

Ernstsen, V., Olsen, P., & Rosenbom, A. E. (2015). Long-term monitoring of nitrate transport to drainage from three agricultural clayey till fields. *Hydrology and Earth System Sciences*, *19*, 3475–3488. https://doi.org/10.5194/hess-19-3475-2015

Fausey, N. R., Brown, L. C., Belcher, H. W., & Kanwar, R. S. (1995). Drainage and water quality in Great Lakes and cornbelt states. *Journal of Irrigation and Drainage Engineering*, *121*, 283–288. https://doi.org/10.1061/(ASCE)0733-9437(1995)121:4(283)

Filipovic, V., Mallmann, F. J. K., Coquet, Y., & Simunek, J. (2014). Numerical simulation of water flow in tile and mole drainage systems. *Agricultural Water Management*, *146*, 105–114. https://doi.org/10.1016/j.agwat.2014.07.020

Ford, W. I., King, K. W., Williams, M. R., & Jr, R. B. C. (2017). Modified APEX model for simulating macropore phosphorus contributions to tile drains. *Journal of Environmental Quality*, *46*, 1413–1423. https://doi.org/10.2134/jeq2016.06.0218

Freeze, R., & Cherry, J. (1979). *Groundwater*. NJ, Prentice-Hall: Englewood Cliffs.

Gardner, J. B., & Drinkwater, L. E. (2009). The fate of nitrogen in grain cropping systems: A meta-analysis of 15n field experiments. *Ecological Applications*, *19*, 2167–2184. https://doi.org/10.1890/08-1122.1

Gentry, L. E., David, M. B., Smith, K. M., & Kovacic, D. A. (1998). Nitrogen cycling and tile drainage nitrate loss in a corn/soybean watershed. *Agriculture Ecosystems and Environment*, *68*, 85–97. https://doi.org/10.1016/S0167-8809(97)00139-4

Gerke, H. H., Dusek, J., Vogel, T., & Kohne, J. M. (2007). Two-dimensional dual-permeability analyses of a bromide tracer experiment on a tile-drained field. *Vadose Zone Journal*, *6*, 651–667.

Gerke, H. H., & van Genuchten, M. T. (1993a). A dual-porosity model for simulating the preferential movement of water and solutes in structured porous media. *Water Resources Philosophy and Phenomenological Research*, *29*(2), 305–319. https://doi.org/10.1029/92WR02339

Gerke, H. H., & van Genuchten, M. T. (1993b). Evaluation of a first-order water transfer term for variably saturated dual-porosity flow models. *Water Resources Philosophy and Phenomenological Research*, *29*(4), 1225–1238. https://doi.org/10.1029/92WR02467

Ginn, T. (1999). On the distribution of multicomponent mixtures over generalized exposure time in subsurface flow and reactive transport: Foundations, and formulations for groundwater age, chemical heterogeneity, and biodegradation. *Water Resources Research*, *35*(5), 1395–1408. https://doi.org/10.1029/1999WR900013

Ginn, T. (2000). On the distribution of multicomponent mixtures over generalized exposure time in subsurface flow and reactive transport: Theory and formulations for residence-time-dependent sorption/desorption with memory. *Water Resources Philosophy and Phenomenological Research*, *36*, 2885–2893. https://doi.org/10.1029/2000WR900170

Goode, D. J. (1996). Direct simulation of groundwater age. *Water Resources Philosophy and Phenomenological Research*, *32*, 289–296. https://doi.org/10.1029/95WR03401

Green, C. H., Tomer, M. D., Luzio, M. D., & Arnold, J. G. (2006). Hydrologic evaluation of the soil and water assessment tool for a large tile-drained watershed in Iowa. *American Society of Agricultural and Biological Engineers*, *49*(2), 413–422.

Guarracino, L. (2007). Estimation of saturated hydraulic conductivity K_s from the van Genuchten shape parameter α. *Water Resources Philosophy and Phenomenological Research*, *43*, 456–465. https://doi.org/10.1029/2006WR005766

Harman, C. J., & Kim, M. (2014). An efficient tracer test for time variable transit time distributions in periodic hydrodynamic systems. *Geophysical Research Letters*, *41*, 1567–1575. https://doi.org/10.1002/2013GL058980

Kim, M., Pangle, L. A., Cardoso, C., Lora, M., Volkmann, T. H. M., Wang, Y., et al. (2016). Transit time distributions and StorAge Selection functions in a sloping soil lysimeter with time-varying flow paths: Direct observation of internal and external transport variability. *Water Resources Philosophy and Phenomenological Research*, *57*, 7105–7129. https://doi.org/10.1002/2016WR018620

Kogbe, J. O. S., & Adediran, J. A. (2003). Influence of nitrogen, phosphorus and potassium application on the yield of maize in the savanna zone of Nigeria. *African Journal of Biotechnology*, *2*, 345–349. https://doi.org/10.1080/00103629509369320

Kohler, A., Abbaspour, K. C., Fritsch, M., van Genuchten, M. T., & Schuline, R. (2001). Simulating unsaturated flow and transport in a macroporous soil to tile drains subject to an entrance head: Model development and preliminary evaluation. *Journal of Hydrology*, *254*, 67–81. https://doi.org/10.1016/S0022-1694(01)00499-1

Kohne, J. M., Kohne, S., & Gerke, H. H. (2002). Estimating the hydraulic functions of dual-permeability models from bulk soil data. *Water Resources Philosophy and Phenomenological Research*, *38*, 1121. https://doi.org/10.1029/2001WR000492

Lavaire, T., Gentry, L. E., & David, M. B. (2017). R. A.Cooke Fate of water and nitrate using drainage water management on tile systems in east-central Illinois. *Agricultural Water Management*, *191*, 218–228. https://doi.org/10.1016/j.agwat.2017.06.004

Le, P. V. V., & Kumar, P. (2014). Power law scaling of topographic depressions and their hydrologic connectivity. *Geophysical Research Letters*, *41*, 1553–1559. https://doi.org/10.1002/2013GL059114

Le, P. V. V., & Kumar, P. (2017). Interaction between ecohydrologic dynamics and microtopographic variability under climate change. *Water Resources Philosophy and Phenomenological Research*, *53*, 8383–8403. https://doi.org/10.1002/2017WR020377

Le, P. V. V., Kumar, P., Valocchi, A. J., & Dang, H.-V. (2015). Gpu-based high-performance computing for integrated surface–sub-surface flow modeling. *Environmental Modeling & Software*, *73*, 1–13. https://doi.org/10.1016/j.envsoft.2015.07.015

Leij, F. J., Alves, W. J., vanGenuchten, M. T., & Williams, J. R. (1996). *The UNSODA unsaturated hydraulic database*. USA: EPA/600/R-96/095, U.S. Environmental Protection Agency Cincinnati, Ohio.

Luo, J., & Cirpka, O. A. (2011). How well do mean breakthrough curves predict mixing-controlled reactive transport? *Water Resources Research*, *47*, W02520. https://doi.org/10.1029/2010WR009461

Madramootoo, C., & Broughton, R. (1987). A computer simulation model of surface and subsurface flows from agricultural areas. *Canadian Water Resources Journal*, *12*(1), 30–43. https://doi.org/10.4296/cwrj1201030

Mohanty, B. P., Bowman, R. S., Hendrickx, J. M. H., & Simunek, M. T. v. J. (1998). Preferential transport of nitrate to a tile drain in an intermittent-flood-irrigated field: Model development and experimental evaluation. *Water Resources Philosophy and Phenomenological Research*, *34*(5), 1061–1076. https://doi.org/10.1029/98WR00294

Mohanty, B. P., Bowman, R. S., Hendrickx, J. M. H., & van Genuchten, M. T. (1997). New piecewise-continuous hydraulic functions for modeling preferential flow in an intermittent-flood-irrigated field. *Water Resources Research*, *33*, 2049–2063.

Nimmo, J. R. (2012). Preferential flow occurs in unsaturated conditions. *Hydrological Processes*, *26*(786–789). https://doi.org/10.1002/hyp.8380

Othmer, H., Diekkruger, B., & Kutilek, M. (1991). Bimodal porosity and unsaturated hydraulic conductivity. *Soil Science*, *152*(3), 139–150. https://doi.org/10.1097/00010694-199109000-00001

Porporato, A., DOdorico, P., Laio, F., & Rodriguez-Iturbe, I. (2003). Hydrologic controls on soil carbon and nitrogen cycles. I. Modeling scheme. *Advance Water Resources*, *26*, 45–58. https://doi.org/10.1016/S0309-1708(02)00094-5

Radcliffe, D. E., Reid, D. K., Blomback, K., Bolster, C. H., Collick, A. S., Easton, Z. M., et al. (2015). Applicability of models to predict phosphorus losses in drained fields: A review. *Journal of Environmental Quality*, *44*(2), 614–628. https://doi.org/10.2134/jeq2014.05.0220

Randall, G. W., & Mulla, D. J. (2001). Nitrate nitrogen in surface waters as influenced by climatic conditions and agricultural practices. *Journal of Environmental Quality*, *30*, 337–44. https://doi.org/10.2134/jeq2001.302337x

Richardson, M., & Kumar, P. (2017). Critical zone services as environmental assessment criteria in intensively managed landscapes. *Earth's Future*, *5*, 617–632. https://doi.org/10.1002/2016EF000517

Rinaldo, A., Beven, K. J., Bertuzzo, E., Nicotina, L., Davies, J., Fiori, A., et al. (2011). Catchment travel time distributions and water flow in soils. *Water Resources Research*, *47*, W07537. https://doi.org/10.1029/2011WR010478

Sands, G. R., Song, I., Busman, L. M., & Hansen, B. J. (2008). The effects of subsurface drainage depth and intensity on nitrate loads in the northern Cornbelt. *Transactions of the ASABE*, *51*(3), 937–946.

Shen, J., Batchelor, W. D., Kanwar, R. S., Jones, J. W., Ritchie, J. T., & Mize, C. W. (1998). Incorporation of a subsurface tile drainage component into a soybean growth model. *American Society of Agricultural Engineers*, *41*(5), 1305–1313.

Simunek, J., & van Genuchten, M. T. (2008). Modeling nonequilibrium flow and transport processes using HYDRUS. *Vadose Zone Journal: 7*, *7*, 782–797. https://doi.org/10.2136/vzj2007.0074

Skaggs, R. W., Breve, M. A., & Gilliamb, J. W. (1994). Hydrologic and water quality impacts of agricultural drainage. *Critical Reviews in Environmental Science and Technology*, *24*(1), 1–32. https://doi.org/10.1080/10643389409388459

Stone, W. W., & Wilson, J. T. (2006). Preferential flow estimates to an agricultural tile drain with implications for glyphosate transport. *Journal of Environmental Quality*, *35*(5), 1825–1835. https://doi.org/10.2134/jeq2006.0068

Turnadge, C., & Smerdon, B. D. (2014). A review of methods for modelling environmental tracers in groundwater: Advantages of tracer concentration simulation. *Journal of Hydrology*, *519*, 3674–3689. https://doi.org/10.1016/j.jhydrol.2014.10.056

Van Alphen, B. J., & Stoorvogel, J. J. (2001). A methodology for precision nitrogen fertilisation in high-input farming systems. *Precision Agriculture*, *2*, 319–332. https://doi.org/10.1023/A:1012338414284

Van Meter, K. J., & Basu, N. B. (2017). Time lags in watershed-scale nutrient transport: An exploration of dominant controls. *Environmental Research Letters*, *12*(084), 017. https://doi.org/10.1088/1748-9326/aa7bf4

Vogel, T., Dohnal, M., & Votrubova, J. (2011). Modeling heat fluxes in macroporous soil under sparse young forest of temperate humid climate. *Journal of Hydrology*, *402*, 367–376. https://doi.org/10.1016/j.jhydrol.2011.03.030

Williams, M. R., King, K. W., Ford, W., Buda, A. R., & Kennedy, C. D. (2016). Effect of tillage on macropore flow and phosphorus transport to tile drains. *Water Resources Research*, *52*, 2868–2882. https://doi.org/10.1002/2015WR017650

Woli, K. P., David, M. B., Cooke, R. A., McIsaac, G. F., & Mitchell, C. A. (2010). Nitrogen balance in and export from agricultural fields associated with controlled drainage systems and denitrifying bioreactors. *Ecological Engineering*, *36*, 1558–1566. https://doi.org/10.1016/j.ecoleng.2010.04.024

Woo, D. K., & Kumar, P. (2016). Mean age distribution of inorganic soil-nitrogen. *Water Resources Philosophy and Phenomenological Research*, *52*, 5516–5536. https://doi.org/10.1002/2015WR017799

Woo, D. K., & Kumar, P. (2017). Role of micro-topographic variability on mean age of soil nitrogen in intensively managed landscape. *Water Resources Philosophy and Phenomenological Research*, *53*, 8404–8422. https://doi.org/10.1002/2017WR021053

Woo, D. K., Quijano, J. C., Kumar, P., Chaoka, S., & Bernacchi, C. J. (2014). Threshold dynamics in soil carbon storage for bioenergy crops. *Environmental Science & Technology*, *48*(20), 12,090–12,098. https://doi.org/10.1021/es5023762

Zarnetske, J. P., Haggerty, R., Wondzell, S. M., & Baker, M. A. (2011). Dynamics of nitrate production and removal as a function of residence time in the hyporheic zone. *Journal of Geophysical Research*, *116*, G01025. https://doi.org/10.1029/2010JG001356

Zhang, W. G., Wilkin, J. L., & Schofield, O. M. E. (2010). Simulation of water age and residence time in new york bight. *Journal of Physical Oceanography*, *40*, 965–982. https://doi.org/10.1175/2009JPO4249.1